

Figure S1 Image features selection using LASSO regression analysis. The LASSO regression coefficient profiles of the (A) CM features and (D) RSTD features. Cross-validation for alpha selection for the (B) CM model and (E) RSTD model. Features weights histograms of the (C) CM model and (F) RSTD model. CI, confidence interval; CM, conventional MRI; LASSO, least absolute shrinkage and selection operator; MRI, magnetic resonance imaging; MSE, mean squared error; RSTD, radiomics and Swin Transformer-based deep learning.

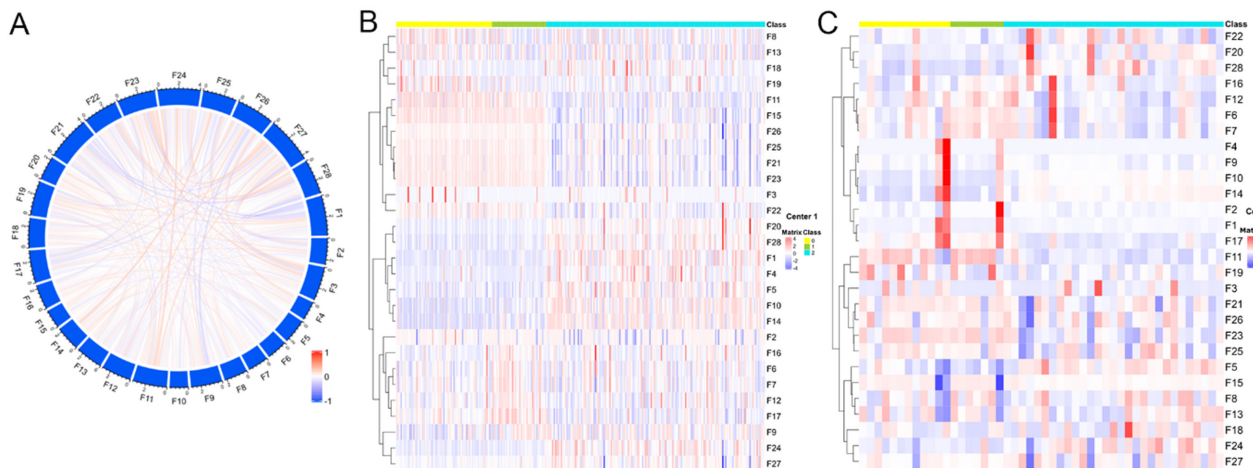


Figure S2 The heatmap of RSTD features. (A) The Person correlation of features in RSTD model showed the correlation between each feature were lower than 0.5 ($P < 0.05$). The heatmap showed the RSTD features distribution among the three subtypes group in Center 1 (B) and Center 2 (C). Center 1, Huashan Hospital; Center 2, The First Affiliated Hospital of Anhui Medical University. Class 0, IDHmut; class 1, IDH-mutant; class 2, IDHwt. IDH, isocitrate dehydrogenase; IDHmut, astrocytoma, IDH-mutant; IDHmut-codel, oligodendroglioma, IDH-mutant and 1p/19q-codeleted; IDHwt, glioblastoma, IDH-wildtype; RSTD, radiomics and Swin Transformer-based deep learning.

Table S1 MRI scan protocol in the Center 1

| 3.0-T MRI systems | Sequences | TR (ms) | TE (ms) | Section thickness (mm) | Intersection gap (mm) | FOV (mm) | Matrix | b value (s/mm ²) |
|-------------------|-----------|-------------|---------|------------------------|-----------------------|----------|---------|------------------------------|
| Siemens Prisma | T1WI | 1,100–1,400 | 8.5–10 | 5 | 5 | 180×240 | 256×163 | – |
| | T2WI | 3,180–5,000 | 99–101 | 5 | 5 | 180×240 | 320×216 | – |
| | FLAIR | 7,500–8,000 | 79–86 | 5 | 5 | 195×240 | 320×182 | – |
| | DWI | 1,600–2,400 | 67 | 5 | 5 | 220×220 | 192×192 | 0, 1,000 |
| | 3D T1C | 1,700 | 2.45 | 1 | 0 | 250×250 | 256×256 | – |
| Siemens Verio | T1WI | 2,000 | 17 | 5 | 5 | 200×230 | 256×256 | – |
| | T2WI | 3,100–3,500 | 95–99 | 5 | 5 | 200×230 | 256×256 | – |
| | FLAIR | 8,000–9,000 | 94–102 | 5 | 5 | 200×230 | 190×250 | – |
| | DWI | 4,900–5,000 | 76–104 | 5 | 5 | 230×230 | 192×192 | 0, 1,000 |
| | 3D T1C | 1,600–2,500 | 2.93 | 1 | 0 | 200×250 | 200×256 | – |
| GE Discovery 750 | T1WI | 1,750–2,385 | 22–24 | 5 | 5 | 240×240 | 288×288 | – |
| | T2WI | 43,000 | 90 | 5 | 5 | 240×240 | 256×256 | – |
| | FLAIR | 8,000–8,525 | 140–146 | 5 | 5 | 240×240 | 256×224 | – |
| | DWI | 3,000 | 65 | 5 | 5 | 240×240 | 256×256 | 0, 1,000 |
| | 3D T1C | 1,850–1,871 | 21–24 | 1 | 0 | 240×240 | 288×288 | – |
| GE Discovery 750W | T1WI | 1,725–1,750 | 7.5–26 | 5 | 5 | 240×240 | 192×256 | – |
| | T2WI | 3,872–4,840 | 102–103 | 5 | 5 | 240×240 | 192×256 | – |
| | FLAIR | 6,600–9,000 | 89–98 | 5 | 5 | 240×240 | 192×256 | – |
| | DWI | 3,228–4,600 | 77–80 | 5 | 5 | 240×240 | 192×256 | 0, 1,000 |
| | 3D T1C | 1,656–1,750 | 20–27 | 1 | 0 | 256×256 | 192×256 | – |

Center 1, Huashan Hospital. 3D T1C, three-dimensional contrast-enhanced T1-weighted; DWI, diffusion-weighted imaging; FLAIR, fluid-attenuated inversion recovery; FOV, field of view; MRI, magnetic resonance imaging; T1WI, T1-weighted image; T2WI, T2-weighted image; TE, echo time; TR, repetition time.

Table S2 MRI scan protocol in the Center 2

| 3.0-T MRI systems | Sequences | TR (ms) | TE (ms) | Section thickness (mm) | Intersection gap (mm) | FOV (mm) | Matrix | b value (s/mm ²) |
|-------------------|-----------|-------------|---------|------------------------|-----------------------|----------|---------|------------------------------|
| Philips Ingenia | T1WI | 2,000 | 15 | 6 | 6 | 240×240 | 232×170 | – |
| | T2WI | 2,501–3,500 | 105–115 | 6 | 6 | 240×240 | 256×256 | – |
| | FLAIR | 6,000 | 120 | 6 | 6 | 240×240 | 240×181 | – |
| | DWI | 2,688–2,711 | 84–86 | 6 | 6 | 240×240 | 152×106 | 0, 1,000 |
| | 3D T1C | 7 | 3 | 1 | 1 | 240×240 | 244×232 | – |
| GE Signa HDxt | T1WI | 1,972–2,287 | 22–26 | 5 | 5 | 198×198 | 320×224 | – |
| | T2WI | 4,480 | 117–119 | 5 | 5 | 187×187 | 384×256 | – |
| | FLAIR | 9,002 | 152–155 | 5 | 5 | 220×220 | 320×192 | – |
| | DWI | 5,600 | 75–76 | 5 | 5 | 220×220 | 160×160 | 0, 1,000 |
| | 3D T1C | 7 | 3 | 1 | 0 | 220×220 | 256×256 | – |
| GE Discovery 750W | T1WI | 1,792–2,242 | 22 | 5 | 5 | 192×192 | 320×224 | – |
| | T2WI | 4,253–6,772 | 101–128 | 5 | 5 | 192×192 | 384×224 | – |
| | FLAIR | 9,000 | 118–120 | 5 | 5 | 192×192 | 256×224 | – |
| | DWI | 4,880 | 77–78 | 5 | 5 | 240×240 | 130×160 | 0, 1,000 |
| | 3D T1C | 7–8 | 3 | 1 | 0 | 208×208 | 256×160 | – |

Center 2, The First Affiliated Hospital of Anhui Medical University. 3D T1C, three-dimensional contrast-enhanced T1-weighted; DWI, diffusion-weighted imaging; FLAIR, fluid-attenuated inversion recovery; FOV, field of view; MRI, magnetic resonance imaging; T1WI, T1-weighted image; T2WI, T2-weighted image; TE, echo time; TR, repetition time.

Table S3 CM features assessment according to VASARI

| MRI features | Category | Definition |
|-----------------------------------|---|---|
| 1. Tumor location | Frontal, temporal, insular, parietal, occipital, others (corpus callosum, basal ganglia, thalamus, brainstem, cerebellum) | Location of lesion geographic epicenter; the largest component of the tumor (either contrast-enhancing tumor or non-enhancing tumor) |
| 2. Tumor size | Centimeter | The longest diameter of the tumor (with both CET and nCET, without edema) |
| 3. Tumor margin | Clear or indistinct | The margin of the surrounding non-enhancing high-signal intensity on FLAIR was recorded as clear or indistinct |
| 4. Enhancement quality | None, mild/minimal, marked/avid | No enhancement. Mild/minimal, barely discernable degree of enhancement relative to pre-contrast images. Marked/avid, Obvious tissue enhancement |
| 5. Proportion enhancing | None, <30%, 30–59%, ≥60% | Proportion of enhancing tumor estimated in the entire tumor volume |
| 6. Proportion necrosis | None, <30%, 30–59%, ≥60% | Proportion of necrosis estimated in the entire tumor volume Necrosis is defined as a region within the tumor that does not enhance or shows markedly diminished enhancement, is high on T2WI, is low on T1WI, and has an irregular border |
| 7. Cyst | Positive or negative | Presence of well defined, rounded regions of very bright T2 signal and low T1 signal essentially matching CSF signal intensity, with very thin, regular, nonenhancing or regularly enhancing walls |
| 8. Multifocal | None, multifocal, multicentric | Multifocal is defined as having at least one region of tumor, either enhancing or nonenhancing, which is not contiguous with the dominant lesion and is outside the region of signal abnormality (edema) surrounding the dominant mass. Multicentric are widely separated lesions in different lobes or different hemispheres that cannot be attributed to one of the previously mentioned pathways |
| 9. T1/FLAIR ratio | Expansive, mixed, infiltrative | Expansive, size of pre-contrast T1 abnormality (exclusive of signal intensity) approximates size of FLAIR abnormality. Mixed, size of T1 abnormality moderately less than FLAIR envelope. Infiltrative, size of pre-contrast T1 abnormality much smaller than size of FLAIR abnormality |
| 10. T2/FLAIR mismatch | Positive or negative | Presence or absence of complete/near-complete hyperintense signal on T2WI, and relatively hypointense signal on FLAIR except for a hyperintense peripheral rim |
| 11. Thickness of enhancing margin | Thin (<3 mm), thick/nodular (≥3 mm), solid | Most of the enhancing rim is thin, regular, and measures <3 mm in thickness and has homogenous enhancement the grade is thin. Most of the rim demonstrates nodular and/or thick enhancement. There is only solid enhancement and no rim, the grade is solid |
| 12. Proportion of edema | None, mild, obvious | No edema. Mild, the maximal diameter of edema < tumor. Obvious, the maximal diameter of edema ≥ tumor |
| 13. Hemorrhage | Positive or negative | Intrinsic hemorrhage in the tumor matrix. Any intrinsic foci of low signal on T2WI or high signal on T1WI (use B0 image if necessary for confirmation) |
| 14. Pial invasion | Positive or negative | Enhancement of the overlying pia in continuity with enhancing or non-enhancing tumor |
| 15. Ependymal extension | Positive or negative | Invasion of any adjacent ependymal surface in continuity with enhancing or non-enhancing tumor matrix |
| 16. Cortical involvement | Positive or negative | Contrast-enhancing tumor or nonenhancing tumor extending to the cortical mantle, or cortex is no longer distinguishable relative to subjacent tumor |
| 17. Deep white matter invasion | Positive or negative | Enhancing or nCET tumor extending into the internal capsule, corpus callosum or brainstem |
| 18. Crosses midline | Positive or negative | Enhancing tissue or nCET crosses into contralateral hemisphere through white matter commissures (exclusive of herniated ipsilateral tissue) |
| 19. Satellites | Positive or negative | A satellite lesion is an area of enhancement within the region of signal abnormality surrounding the dominant lesion but not contiguous in any part with the major tumor mass |
| 20. Restricted diffusion | Positive or negative | Restricted diffusion (high signal on DWI and low signal on ADC map) in the enhancing or nCET portion of the tumor |

Details of qualitative imaging analyses can be seen on the following site: <https://wiki.cancerimagingarchive.net/display/Public/VASARI+Research+Project>. CET, contrast-enhancing tumor; CM, conventional MRI; CSF, cerebrospinal fluid; DWI, diffusion-weighted imaging; FLAIR, fluid-attenuated inversion recovery; MRI, magnetic resonance imaging; nCET, non-CET; T1WI, T1-weighted image; T2WI, T2-weighted image; VASARI, Visually Accessible Rembrandt Images.

Table S4 The hyperparameter optimization of ML algorithms in model development

| ML model | Best model parameters | | |
|----------|---|--|--|
| | CM model | RSTD model | Combined model |
| kNN | Algorithm: kd_tree, n_neighbors: 3, weights: distance | Algorithm: kd_tree, n_neighbors: 1, weights: uniform | Algorithm: auto, n_neighbors: 8, weights: distance |
| LightGBM | Learning_rate: 0.321, max_depth: 1, n_estimators: 5 | Learning_rate: 0.436, max_depth: 7, n_estimators: 47 | Learning_rate: 0.126, max_depth: 9, n_estimators: 8 |
| RF | Max_depth: 2, min_samples_split: 4, n_estimators: 38 | Max_depth: 4, min_samples_split: 4, n_estimators: 46 | Max_depth: 4, min_samples_split: 9, n_estimators: 16 |
| SVM | C: 1.0, kernel: rbf, gamma: auto | C: 1.0, kernel: kernel, gamma: auto | C: 1.0, kernel: rbf, gamma: auto |
| SGD | Alpha: 0.01, loss: log_loss, penalty: 12 | Alpha: 0.01, loss: log_loss, penalty: 12 | Alpha: 0.01, loss: log_loss, penalty: 12 |
| XGBoost | N_estimators: 26, max_depth: 3, learning_rate: 0.243 | N_estimators: 32, max_depth: 3, learning_rate: 0.376 | N_estimators: 40, max_depth: 1, learning_rate: 0.441 |

The GPU system used in this study is the NVIDIA Tesla P40, which has 22.5 GB of dedicated memory. CM, conventional MRI; kNN, k-nearest neighbor; LightGBM, light gradient-boosting machine; ML, machine learning; MRI, magnetic resonance imaging; RF, random forest; RSTD, radiomics and Swin Transformer-based deep learning; SGD, stochastic gradient descent; SVM, support vector machine; XGBoost, extreme gradient boosting.

Table S5 Selected features for the CM and RSTD models

| Model | Name | Feature |
|---|---------------------|--|
| CM model (6 features) | Location | Tumor location |
| | Equality | Enhancement quality |
| | Eproportion | Proportion enhancing |
| | Ethickness | Thickness of enhancing margin |
| | EpendymalExtension | Ependymal extension |
| | CorticalInvolvement | Cortical involvement |
| RSTD model (28 Radiomics features features) | F1 | Original_firstorder_MeanAbsoluteDeviation |
| | F2 | Original_glcml_ClusterShade |
| | F3 | Original_ngtdm_Contrast |
| | F4 | Log-sigma-1-mm-3D_firstorder_TotalEnergy |
| | F5 | Log-sigma-1-mm-3D_glrIm_LongRunLowGrayLevelEmphasis |
| | F6 | Log-sigma-1-mm-3D_glrIm_RunLengthNonUniformityNormalized |
| | F7 | Log-sigma-1-mm-3D_glrIm_ShortRunEmphasis |
| | F8 | Log-sigma-1-mm-3D_glszm_GrayLevelNonUniformityNormalized |
| | F9 | Log-sigma-1-mm-3D_glszm_GrayLevelVariance |
| | F10 | Log-sigma-1-mm-3D_glszm_HighGrayLevelZoneEmphasis |
| | F11 | Log-sigma-1-mm-3D_glszm_LowGrayLevelZoneEmphasis |
| | F12 | Log-sigma-2-mm-3D_glrIm_ShortRunEmphasis |
| | F13 | Log-sigma-2-mm-3D_glszm_GrayLevelNonUniformityNormalized |
| | F14 | Log-sigma-2-mm-3D_glszm_HighGrayLevelZoneEmphasis |
| | F15 | Log-sigma-3-mm-3D_firstorder_10Percentile |
| | F16 | Log-sigma-3-mm-3D_glrIm_RunLengthNonUniformityNormalized |
| | F17 | Log-sigma-3-mm-3D_glrIm_ShortRunHighGrayLevelEmphasis |
| | F18 | Log-sigma-3-mm-3D_glszm_SizeZoneNonUniformity |
| | F19 | Log-sigma-3-mm-3D_glszm_SmallAreaLowGrayLevelEmphasis |
| Swin Transformer-based deep learning features | | |
| F20 | Column_97 | |
| F21 | Column_134 | |
| F22 | Column_217 | |
| F23 | Column_434 | |
| F24 | Column_460 | |
| F25 | Column_655 | |
| F26 | Column_895 | |
| F27 | Column_998 | |
| F28 | Column_1003 | |

CM, conventional MRI; MRI, magnetic resonance imaging; RSTD, radiomics and Swin Transformer-based deep learning.